

Periodicities in an active region correlated with Type III radio bursts observed by Parker Solar Probe

Cynthia Cattell¹, Lindsay Glesener¹, Benjamin Leiran¹, Keith Goetz¹, Juan Carlos Martínez Oliveros², Samuel T. Badman^{2,3}, Marc Pulupa², and Stuart D. Bale^{2,3}

¹ School of Physics and Astronomy, University of Minnesota, 116 Church St. SE Minneapolis, MN 55455 USA
e-mail: cattell@umn.edu

² Space Sciences Laboratory, University of California, Berkeley, Berkeley, CA 94709 USA

³ (Department of Physics, University of California, Berkeley, Berkeley, CA 94709

Received ; accepted

ABSTRACT

Context. Periodicities have frequently been reported across many wavelengths in the solar corona. Correlated periods of ~ 5 minutes, comparable to solar p-modes, are suggestive of coupling between the photosphere and the corona.

Aims. Our study investigates whether there are correlations in the periodic behavior of Type III radio bursts, indicative of non-thermal electron acceleration processes, and coronal EUV emission, assessing heating and cooling, in an active region when there are no large flares.

Methods. We use coordinated observations of Type III radio bursts from the FIELDS instrument on Parker Solar Probe (PSP), of extreme ultraviolet emissions by the Solar Dynamics Observatory (SDO)/AIA and white light observations by SDO/HMI, and of solar flare x-rays by Nuclear Spectroscopic Telescope Array (NuSTAR) on April 12, 2019. Several methods for assessing periodicities are utilized and compared to validate periods obtained.

Results. Periodicities of ~ 5 minutes in the EUV in several areas of an active region are well correlated with the repetition rate of the Type III radio bursts observed on both PSP and Wind. Detrended 211Å and 171Å light curves show periodic profiles in multiple locations, with 171Å peaks lagging those seen in 211Å. This is suggestive of impulsive events that result in heating and then cooling in the lower corona. NuSTAR x-rays provide evidence for at least one microflare during the interval of Type III bursts, but there is not a one-to-one correspondence between the x-rays and the Type-III bursts. Our study provides evidence for periodic acceleration of non-thermal electrons (required to generate Type III radio bursts) when there were no observable flares either in the x-ray data or the EUV. The acceleration process, therefore, must be associated with small impulsive events, perhaps nanoflares.

Key words. Radiation mechanisms: non-thermal, Waves, Plasma, Magnetic reconnection, Sun: corona, Sun: oscillations, Sun: radio radiation, Sun: UV radiation

1. Introduction

Quasi-periodic variations with periods ranging from seconds to tens of minutes have long been reported for many phenomena in the active and quiescent solar corona, starting from the first detection of correlated periodicities in solar flare x-rays and microwaves (Parks & Winckler 1969). Examples include rapid variations in Type III radio bursts (Mangeney and Pick, 1989; Ramesh et al., 2005). In the extreme ultraviolet (EUV), the extensive observations of these periodicities, often interpreted as the signature of magnetohydrodynamic (MHD) waves, have led to the development of coronal seismology, to assess properties of the corona (Nakariakov & Verwichte 2005; Kupriyanova et al. 2020; Roberts et al. 1984; Roberts 2000; De Moortel & Nakariakov 2012). Long-lived 3 to 5 minute pulsations are also observed in sunspots (Sych et al. 2012; Battams et al. 2019; Sych et al. 2020). Quasi-periodic variations in x-rays and gamma-rays from solar and stellar flares are also observed (Van Doorselaere et al. 2016; Kupriyanova et al. 2020; Inglis et al. 2015; Dennis et al. 2017; Hayes et al. 2020).

Several studies have described correlated periodicities in various combinations of Type III radio bursts, hard x-rays, EUV emissions, microwaves, and sunspots at periods of minutes. Type III bursts are of particular interest because they provide informa-

tion on acceleration of non-thermal electron beams. Innes et al. (2011) reported correlations between ~ 3 minute periodicities in Type III radio bursts and coronal jets observed in 211 Å, which were possibly related to 3-minute oscillations in sunspot brightness. Most other studies have described periodicities in association with large flares. Oscillations in Type III radio waves, hard x-rays, and jets at ~ 4 minute periods were reported by Li et al. (2015). Kumar et al. (2016) found ~ 3 minute pulsations in hard x-rays, microwave emission, Type III bursts and a nearby sunspot.

Foullon et al. (2010) found periods of ~ 10 minutes in Type IIIs and x-rays, with longer ~ 18 minute periods in the few GHz radio emissions (interpreted as due to non-thermal gyroresonance). Shorter periods (~ 100 s) were reported by Kumar et al. (2017) in correlations between coronal fast mode waves, Type III and IV radio bursts, microwaves, and thermal x-rays. Kupriyanova et al. (2016) described ~ 40 s variations in hard x-rays, microwaves and Type III waves, consistent with modulation of non-thermal electron acceleration, but not thermal processes.

Explanations for the periodicities include MHD waves (Alfvén waves and fast or slow mode magnetosonic waves), modulation of reconnection at flare sites via intrinsic pro-

cesses, current sheet structure (De Moortel & Nakariakov 2012; McLaughlin et al. 2018; Aschwanden 2006), or coupling of solar p-modes to coronal waves (Zhao et al. 2016). For events that include non-thermal x-rays and/or Type III radio bursts, periodicities are most often attributed to modulated reconnection. Theoretical and modeling studies of reconnection with periodicities, which can be due to intrinsic loading/unloading timescales, modulation by MHD waves, or other processes, include Murray et al. (2009); McLaughlin et al. (2012); Thurgood et al. (2017). An alternate approach attributes quasi-periodic behavior to stochastic processes (Veronig et al. 2000; Aschwanden et al. 2016; Eastwood et al. 2009).

In this report, we describe observations of repetitive Type III bursts observed by Parker Solar Probe (PSP) on April 12, 2019, and their correlation with periodic rapid heating and cooling in the 211 Å and 171 Å bandpass filters (~ 2 MK and ~ 0.6 MK peak temperature responses, respectively) on the Solar Dynamics Observatory (SDO) / Atmospheric Imaging Assembly (AIA). Section 2 describes the data sets and analysis techniques; Section 3 shows the observations; and Section 4 discusses the results, comparisons to other studies and interpretation in terms of possible physical models.

2. Data sets

We focus on an interval on April 12, 2019, when simultaneous data were obtained by NuSTAR, PSP, Wind, and SDO. Radio data were obtained with the Radio Frequency Spectrometer (RFS)(Pulupa et al. 2017), part of the PSP FIELDS suite (Bale et al. 2016). This interval is at the end of the second encounter, so the sample rate was low, ~ 1 sample per 55 s. We also examined higher rate (1 sample per 7 s) data for intervals with similar periodic bursts. We also utilize radio data from Wind/Waves (Bougeret et al. 1995), from RAD1 (20-1040 kHz) and RAD2 (1.075-13.825 MHz) at 1 sample per 16 s.

Extreme ultraviolet data from SDO/AIA (Lemen et al. 2012) and magnetic field information from the Helioseismic and Magnetic Imager (HMI; Schou et al. 2012) are utilized to examine periodicities and solar structures. AIA data were obtained in 7 wavelengths at a 12 s cadence over the full sun. Analysis of AIA data is focused on five areas within active region 12738 (NOAA designation).

During the interval of interest, based on field line tracing using a combination of the Potential Field Source Surface model and the Parker spiral (see Badman et al. (2020) for a description of the method), PSP and Wind both map closer to the smaller active region near 60 degrees longitude, which was not observable by SDO at this time. Harra et al. (2020) study this smaller active region (AR 12737) and conclude from the dynamics that it may be contributing to the population of Type III bursts observed, although they study an earlier interval from March 31-April 6th, during which time AR 12738 was behind the limb as viewed from Earth. PFSS mapping also suggests that there was no direct magnetic connection to either active region and thus no in situ observations of electron beams are expected (or indeed observed) at PSP or Wind. One study (Krupar et al. 2020) used radio triangulation with STEREO and Wind to show that in at least one case study of a large type III burst, the electron beam appears to be consistent with a Parker spiral emerging from AR 12378. Pulupa et al. (2020), who examined the full encounter, also associated the bursts with AR 12738, citing the consistency of the orientation of its bipole on the solar disk with the polarization of radio emission measured in situ (although this is also true of AR 12737 since it is in the same solar hemisphere in the

same solar rotation). The observations of Krupar et al. (2020) and Pulupa et al. (2020) suggest that our comparison of the Type III bursts to periodicities in AR 12738 is appropriate.

On April 12 and April 13, 2019, at the end of the second PSP periastron pass, NuSTAR observed the sun, measuring hard X-rays at energies from 2.5 to 10 keV for six subintervals when PSP obtained radio data. Several GOES A7 to A9 class flares were seen in each of the two intervals on April 12 for which there are PSP radio data, and two B class flares on April 13 with PSP radio data. See Figures 1, 2, and 3 for summaries of the observations.

3. Observations

An overview of the event is shown in Figure 1, including the x-ray data from GOES-14 (panel a), the Type III radio bursts seen on Wind (panel b) and PSP/FIELDS (panel c). During the interval from 540 UT to 1230 UT, all PSP instruments were turned off to enable high rate science data downlink. The quasi-periodic repetition of the Type III radio bursts seen by both PSP and Wind is clear, with periods of ~ 4 to 5 minutes. Note that similar bursts are observed intermittently for ~ 10 days from either or both of PSP and Wind. The interval displays some characteristics of a Type III radio storm (Fainberg & Stone 1970; Bougeret et al. 1984; Morioka et al. 2007). The individual bursts are lower power and have a more limited frequency range than flare-associated Type IIIs. The repetition rate is longer than the range found for storms (~ 10 s to 1 minute); however, this may be due to the low level of solar activity. Pulupa et al. (2020) characterized the properties of the Type III bursts for two intervals, one before our observations (April 3 08 UT to April 4 08 UT), and one after (April 17 17:00 UT to April 18 05:00 UT), and concluded the Type IIIs were associated with Type III storms.

To examine possible correlations between the low corona (as probed by AIA) and the Type III radio bursts, we focus on the interval between 1715 and 18:45 UT. Figure 2 plots the PSP radio data, the NuSTAR x-rays, and the GOES x-rays together, with PSP times shifted to 1 AU. Although the flares do occur during times of intense radio activity and the X-ray bursts may be related to the radio bursts, there is not a one-to-one correspondence between the flare x-ray emissions(c and d) and the Type III bursts.

SDO/AIA measures EUV emission from the Sun in passbands defined by ten filters, six of which are sensitive to coronal temperatures (Lemen et al. 2012). Images are full-Sun at 1.2 arcsec resolution and a 12 s cadence for each filter. Several diverse regions of active region 12738 were selected for individual analysis, including the region at the major sunspot, regions where small transients were visible by eye, and some quiet regions. Regions are shown in Figure 3. Within each of these regions, AIA emission in individual filters was totaled over the region and plotted as a function of time. These included all of the coronal filters as well as the 304Å filter, which is sensitive to the He II ions typically found in the chromosphere and transition region. Solar rotation was not removed, so the solar emission drifts across each region at a slow rate (~ 10 arcsec per hour). Some regions exhibited a periodic behavior to their time profiles in addition to macroscopic, transient events. The time profiles were detrended so that this periodic behavior was more apparent, as shown in Figure 4, panels (d) and (e). Detrending was performed by subtracting a smoothed curve (with a running average over 10 minutes) from each time profile.

Figure 3 shows the active region with the five subregions indicated. The top panels are images of 211 Å and 171 Å from

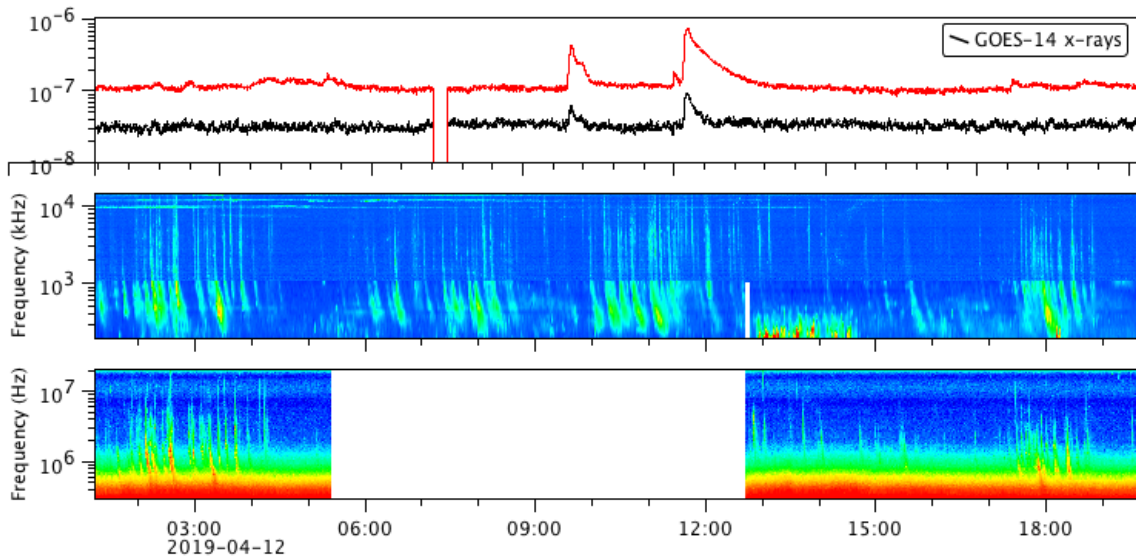


Fig. 1. Overview of (top) x-rays observed by GOES-14, and Type III radio bursts (300 kHz to 20 MHz) observed by (middle) Wind and (bottom) Parker Solar Probe for April 12, 2019 0100 to 2000 UT. Times are those at which the emission was recorded on the respective spacecraft; the PSP times have not been shifted to 1 AU.

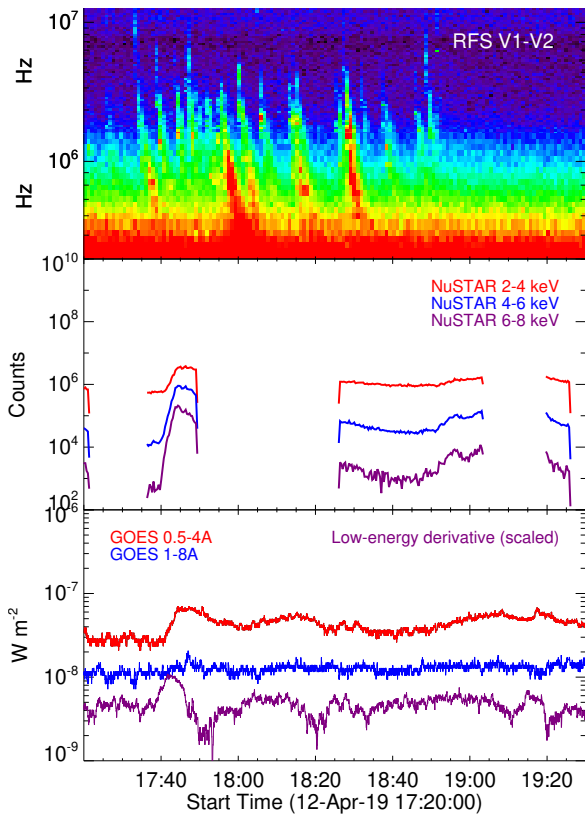


Fig. 2. Interval of interest from 17:20 to 19:30 UT. The top panel shows PSP/FIELDS radio data (V12), with times propagated to 1 AU. The middle panel shows the NuSTAR x-ray data, and the bottom panel shows the GOES x-ray data.

AIA, and the bottom panels are the line-of-sight (LOS) magne-

togram and intensity map from HMI. For the EUV images, our study utilizes bandpass filter images, and as such examines only periodicity in the EUV bandpass brightnesses, and not in other properties such as line Doppler velocity or Doppler width.

The EUV and radio data were examined for periodicities utilizing a method that identified peaks and valleys above a threshold value in the normalized power (PSP and Wind) or normalized detrended light curve (SDO/AIA and HMI). The detrending time periods and intervals for analysis of AIA data were selected to avoid introducing artificial periods (Auchère et al. 2016; Dominique et al. 2018). Periodicities for the radio data were determined both using the measured values and using data interpolated to the cadence of the AIA data. Figure 4 shows an example of the ‘peak’ approach for the radio, EUV and HMI data sets. Panels a and b show the normalized power above average for the two frequency bands (6.2 MHz and 18.4 MHz) from the PSP radio data versus time. Panel c plots the resulting average periods versus frequency for the HFR (>5 MHz) band, determined using a threshold of 1 for the normalized power. Panels d and e plot the detrended normalized intensity for two AIA bands, 171 Å and 211 Å in Region 2; and panel f plots the average period versus temperature (based on the peak of the temperature responses of each bandpass for the six coronal lines and the one photospheric line) for Region 2, where the periodicities were most prominent. The AIA temperature responses are overplotted; colors identify the same lines for both periodicity and temperature response. It should be noted that all of the AIA bandpass filters have broad temperature responses, and some have bimodal responses. We cannot use these data to measure a strict temperature without differential emission measure analysis, but the peak temperature response gives a rough estimate of which temperature range we are likely to be observing. For the filters that have a doubly peaked response, we have plotted the temperatures of both peaks for reference. Although some studies of quasi-periodicities in EUV lines have identified a temperature dependence, the periods we observe are independent of temper-

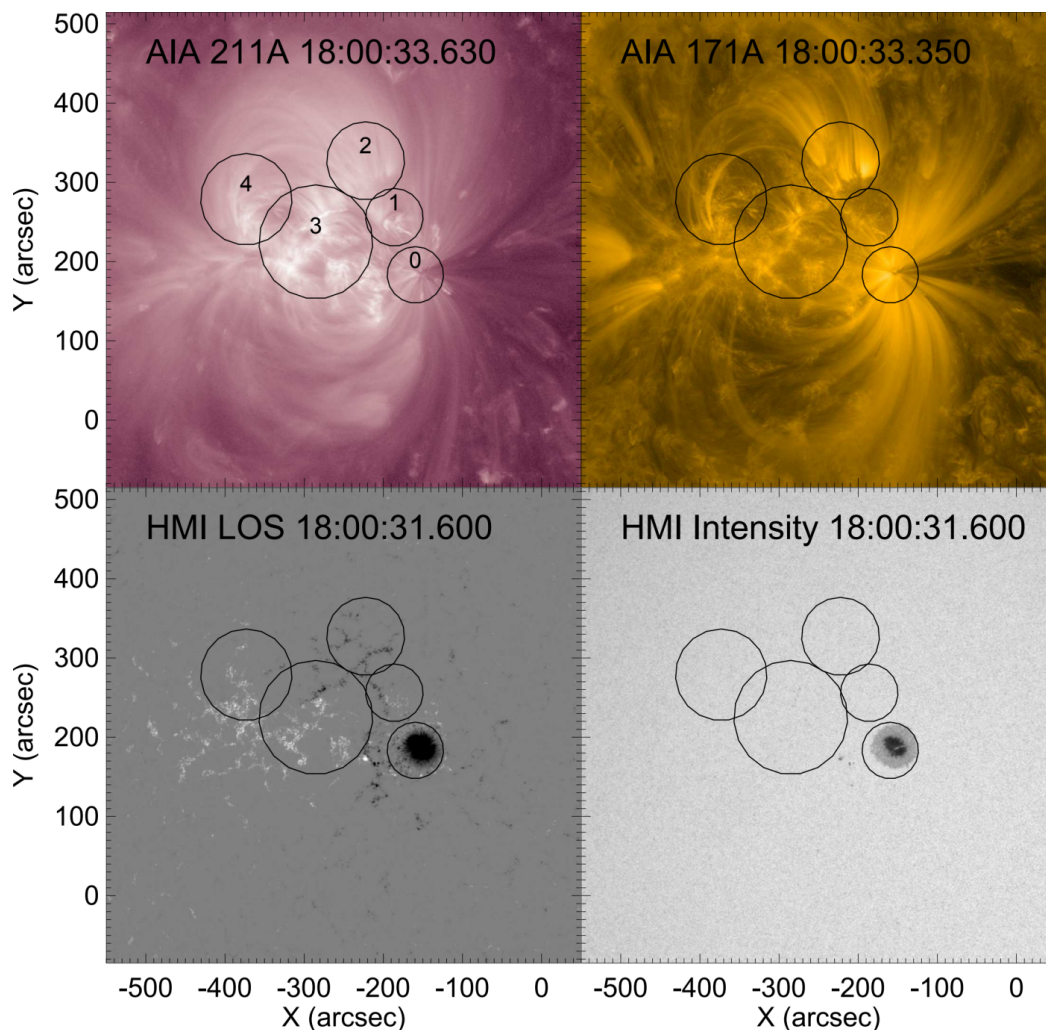


Fig. 3. Regions analyzed are shown overlaid on SDO images. The top row includes two AIA filters that have sensitivity to quiescent coronal temperatures, and the bottom row includes the HMI line-of-sight magnetogram and intensity map. Images shown are at a time near the middle of the analyzed interval. At the latitude of this active region, solar rotation causes sources to drift westward at a rate of about 10 arcsec per hour.

ature to within the error bars. Panels g and h plot the time series of the HMI intensity for 2 regions within the EUV subregion 0, and the periods determined for all 3 HMI regions are plotted in panel i. It is clear that the periodicity in the radio waves (~ 4 -5 minutes) is comparable to those in the AIA and HMI data. The behavior of the EUV emission in the other 4 regions was also examined (not shown); similar periodicities were observed but the amplitude of the variations was smaller. Note that periodicities in the radio, EUV and HMI data were also determined using fast Fourier transforms (FFTs), with similar results. We have also examined periodicities in the PSP radio data for intervals with similar repetitive Type III bursts earlier in this pass when higher rate data were obtained. Figure 5 (same format as Figure 4) shows that the periodicities observed in the Type IIIs are very stable, and are observed for many days. Repetitive Type III radio bursts observed by PSP earlier in this encounter are discussed by (Harra et al. 2020).

The correlation between the times series of the PSP radio data and the SDO/EUV data is shown in Figure 6, in which the 171 Å (in red) and 211 Å (in white) detrended light curves are plotted on top of the PSP radio power. The radio data have been time-shifted to account for propagation from the solar radial position of PSP to 1 AU. For the first radio bursts, the typical timing

observed is that the radio burst is followed by 211 Å emission, with the 171 Å emission increasing as the 211 Å decreases. For most events, the rise in 211 Å precedes that in the 171 Å. This is suggestive of rapid heating, followed by rapid cooling. A possible interpretation is that the heating is due to electrons accelerated downward in the small-scale reconnection that accelerates electrons upward to generate the radio waves.

4. Discussion

Many different mechanisms have been proposed to explain observed periodic and quasi-periodic behavior in the EUV and radio data. Our study provides evidence for periodic acceleration of non-thermal electrons (required to generate Type III radio bursts) when there were no observable flares either in the x-ray data or the EUV. The occurrence of Type III bursts without significant flaring was also observed by (Harra et al. 2020) earlier in this PSP encounter. The acceleration process, therefore, must be associated with small impulsive events (perhaps nanoflares) (Viall & Klimchuk 2011; Bradshaw et al. 2012; Ishikawa et al. 2017; Hudson 1991; Klimchuk 2015), or with some other mechanism such as kinetic Alfvén waves (McClements & Fletcher 2009). Small acceleration events have also been seen as isolated

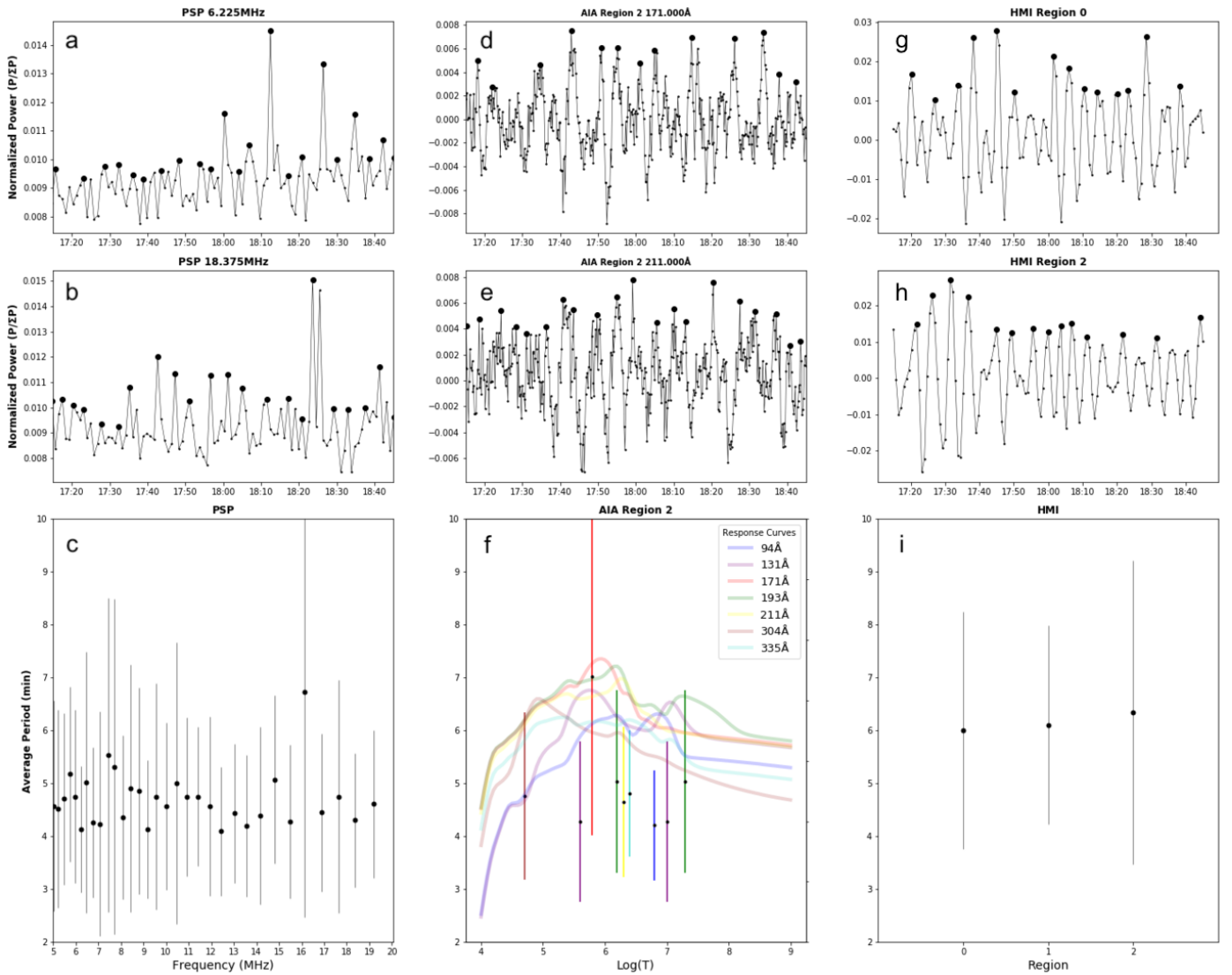


Fig. 4. Periodicities in PSP/FIELDS HFR radio power, AIA emission in Region 2 (as defined in 3), and HMI intensity. (a) 6.225 MHz and (b) 18.375 MHz interpolated normalized power with black dots indicating the identified peaks; (c) periods identified for all frequencies > 5 MHz; (d) AIA 171 Å and (e) 211 Å detrended normalized intensity with black dots indicating the identified peaks; and (f) periods identified for all AIA passbands in Region 2, versus wavelength with temperature response curves overplotted; (g) and (h) HMI emission in two regions; and (i) periods identified in HMI data. For panels (d) and (e), the AIA lightcurves have been detrended. The units are residual data numbers (DNs) after a 10-minute average curve was subtracted. In panel (f), the temperatures of the data points are those listed in Table 1 of (Lemen et al. 2012) for each passband (these are approximately the peaks of the temperature responses), but the colored lines show the temperature responses themselves, in arbitrary units, to give a better representation of possible temperatures for each data point. When more than one temperature is listed in Table 1 of (Lemen et al. 2012), we have included a data point for both, since we cannot distinguish them.

events (James et al. 2017) with a Type III burst and only very weak hard x-rays. If the mechanism is nanoflares, the electron acceleration may involve processes seen in flares (e.g. those described in Zharkova et al. (2011)). Studies of small microflares using NuSTAR have provided evidence for acceleration of non-thermal electrons at energies below 7 keV (Glesener et al. 2020), with significant collisional energy deposition that could provide heating of the corona. Studies have predicted a range of periodicities for nanoflares (Viall & Klimchuk 2011; Bradshaw et al. 2012; Klimchuk 2015; Knizhnik & Reep 2020) depending on parameters such as cooling rates.

One possibility for obtaining periodicities is that MHD waves in the corona can initiate magnetic field reconfiguration, resulting in small-scale reconnection. It has been shown that

propagating coronal waves can destabilize active regions (e.g. Ofman & Thompson 2002). There are many cases of fast mode waves observed in the low corona in association with eruptions (Veronig et al. 2011; Liu et al. 2018), but there has been less work on this phenomena at quiet times. Another possibility is that waves generated by the field reconfiguration propagate through the active region with a temperature-dependent dispersion, for example via fast mode waves. For the fast mode (or any other temperature-dependent mode), the observed frequencies would differ in the AIA filters. There was no clear temperature dependence in the periodicities for our event, suggesting that this mechanism was not operating. Magnetic field reconnection may also occur in an inherently periodic fashion (Van Doorselaere et al. 2016; Nakariakov & Melnikov 2009). In this case,

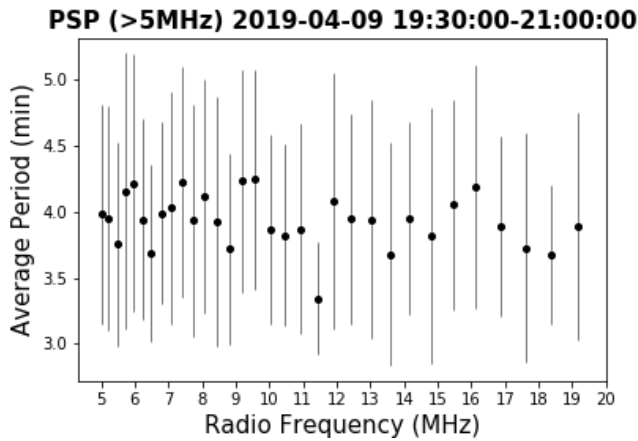


Fig. 5. Periodicities seen in PSP radio for earlier interval with higher data rate.

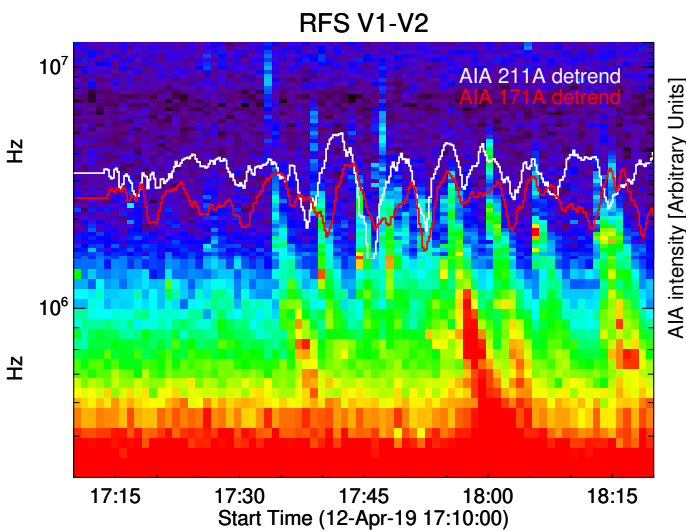


Fig. 6. Time series of PSP radio with detrended AIA 211 (white) and 171 (red) overplotted for Region 2. PSP times have been propagated to 1 AU.

the AIA emission represents the heating and cooling associated with these periodic reconnection events, and all the AIA filters, as well as the radio data, should exhibit the same frequency, as was the case in our event.

It is possible for the photosphere to be the ultimate source of the periodicity in either case. De Moortel et al. (2002) found different oscillation periods for coronal loops with footpoints inside sunspots than for ones with footpoints outside sunspots. They concluded that the waves were not associated with flares, but rather with a driver whose effects propagated up through the transition region. Correlations observed by Li et al. (2015) between soft x-rays and EUV jets at ~ 5 minute periods led them to suggest that photospheric p-modes may lead to periodic reconnection in the corona. De Pontieu et al. (2005) modeled magnetic flux tubes and showed that 5 minute p-mode waves propagated into the corona, and could thus be the source of 5 minute periodicities in coronal wavelengths. The possibility that the photosphere is the source of the periodicity we observe is consistent with the correlation of the Type III bursts and the EUV with the HMI brightness.

A definitive determination of whether the periodicities in the EUV observed in our event were due to MHD waves, periodic jetting or another process would require analysis of more complex properties in the AIA data, such as Doppler velocity (De Pontieu & McIntosh 2010; Kupriyanova et al. 2020; De Moortel & Nakariakov 2012). Liu & Ofman (2014) review identification of wave modes in the AIA data, including fast mode waves, Kelvin-Helmholtz waves, and ‘mini EUV-waves.’ The latter may be relevant for our observations as they represent small-scale, weaker waves that occur more often than larger waves.

Some studies of periodicities of minutes have concluded that modulation of reconnection due to current sheet oscillations is most consistent with their observations (Kupriyanova et al. 2016), and that the height over which modulated processes occur is inconsistent with MHD waves. Other mechanisms for producing modulated reconnection have been investigated by many researchers. (Nakariakov et al. 2006) discuss enhanced reconnection associated with kinetic instabilities driven by currents associated with fast mode waves and the interaction of magnetic loops. Liu et al. (2011) found 3 minute fast mode waves correlated with flare QPP, implying a causal link via wave modulation of reconnection. In a study of ~ 10 -20s QP in flares and radio waves, (Fleishman et al. 2008) compared properties to two models, effects of MHD waves on radio emissions and QP injections of electrons, and concluded that the latter better fit their observations.

Our observations are qualitatively similar to those reported by (Innes et al. 2011), although those observations centered on very clearly distinguishable, prominent jets. In the event described herein, periodic behavior is observed most clearly in the 211 Å passband (the same as in the Innes study) but jet behavior is less prominent. There are certainly many jets occurring in the active region, but the EUV oscillations are not limited to one jet-producing region. Similar periodicities occur throughout the active region. Li et al. (2015) described recurrent jets associated with magnetic flux cancellation and periodic, 5 and 13 minutes, brightenings in the EUV at the jet base. They concluded that their observations were consistent with modulated reconnection. McIntosh & De Pontieu (2009) provide evidence for 3 to 5 minute periodicities in weak upflows in the transition region in the quiet sun, which may be linked to similar coronal periodicities.

A very different explanation sometimes put forth for quasi-periodic behavior in flares and Type III radio ‘storms’ is based on avalanche or chaos models (Eastwood et al. 2009; Isliker et al. 1998). In a study of two other intervals in this PSP encounter, Pulupa et al. (2020) found that the power law index of intensity distribution was consistent with (Eastwood et al. 2009). They found that the waiting time distribution dependence on frequency differed in the two intervals, discussed possible reasons, and comparisons to other studies. Type III storms with very low amplitude and frequent bursts (~ 800 /hour) have been reported by Tun Beltran et al. (2015) using high time resolution ground-based instruments. They propose that continuous reconnection in the corona in concert with density and temperature inhomogeneities may explain their observations. Studies have predicted a range of periodicities for nanoflares (Viall & Klimchuk 2011; Bradshaw et al. 2012; Klimchuk 2015) depending on parameters such cooling rates. MHD simulations of the time intervals between nanoflare reconnection. Knizhnik & Reep (2020) showed a power law distribution, similar to the conclusion of Eastwood et al. (2009) for Type III storms. The time intervals we observed between acceleration events are very consistent over many day

intervals, and thus not explainable by a process resulting in a power law distribution.

We have reported the first observations of periodic Type III radio bursts by Parker Solar Probe and their correlation with periodic rapid heating and cooling in an active region in several EUV channels of the SDO/AIA, and with variations in sunspot brightness seen in the SDO/HMI. The periods were ~ 5 minutes in all wavelengths, and comparable to solar p-modes. Similar Type III bursts were also observed by WIND. NuSTAR hard x-rays occurred in association with at least one small microflare in the active region, but were not directly correlated with the Type III bursts. Because Type III radio bursts are generated by non-thermal electrons, this event provides strong evidence for quasi-periodic small-scale acceleration processes in the corona during quiet times. The periodic Type III bursts were observed for days, suggesting that these periodic electron acceleration events may be important for understanding coronal heating.

Acknowledgements. We acknowledge the NASA Parker Solar Probe Mission, and the FIELDS team led by S. D. Bale, and the SWEAP team led by J. Kasper for use of data. The FIELDS experiment on the Parker Solar Probe spacecraft was designed and developed under NASA contract NNN06AA01C, and data analysis at UMN and UCB was supported under the same contract. Work at UMN was also supported by the NASA SolFER Drive Science Center (grant 80NSSC20K0627) and the NASA NuSTAR Guest Observer program (grant 80NSSC18K1744). S.T.B. was supported by NASA Headquarters under the NASA Earth and Space Science Fellowship Program Grant 80NSSC18K1201

References

- Aschwanden, M. 2006, *Physics of the solar corona* (Springer Science & Business Media)
- Aschwanden, M. J., Crosby, N. B., Dimitropoulou, M., et al. 2016, *Space Science Reviews*, 198, 47
- Auchère, F., Froment, C., Bocchialini, K., Buchlin, E., & Solomon, J. 2016, *The Astrophysical Journal*, 825, 110
- Badman, S. T., Bale, S. D., Martínez Oliveros, J. C., et al. 2020, *The Astrophysical Journal Supplement Series*, 246, 23
- Bale, S. D., Goetz, K., Harvey, P. R., et al. 2016, *Space Science Reviews*, 204, 49
- Battams, K., Gallagher, B. M., & Weigel, R. S. 2019, *Sol. Phys.*, 294, 11
- Bougeret, J.-L., Fainberg, J., & Stone, R. 1984, *Astronomy and Astrophysics*, 136, 255
- Bougeret, J.-L., Kaiser, M. L., Kellogg, P. J., et al. 1995, *Space Science Reviews*, 71, 231, publisher: Springer
- Bradshaw, S. J., Klimchuk, J. A., & Reep, J. W. 2012, *The Astrophysical Journal*, 758, 53
- De Moortel, I., Ireland, J., Hood, A. W., & Walsh, R. W. 2002, *Astronomy & Astrophysics*, 387, L13
- De Moortel, I. & Nakariakov, V. M. 2012, *Philosophical Transactions of the Royal Society A: Mathematical, Physical and Engineering Sciences*, 370, 3193
- De Pontieu, B., Erdélyi, R., & De Moortel, I. 2005, *The Astrophysical Journal Letters*, 624, L61, publisher: IOP Publishing
- De Pontieu, B. & McIntosh, S. W. 2010, *The Astrophysical Journal*, 722, 1013
- Dennis, B. R., Tolbert, A. K., Inglis, A., et al. 2017, *ApJ*, 836, 84
- Dominique, M., Zhukov, A. N., Dolla, L., Inglis, A., & Lapenta, G. 2018, *Solar Physics*, 293
- Eastwood, J., Wheatland, M., Hudson, H., et al. 2009, *The Astrophysical Journal Letters*, 708, L95
- Fainberg, J. & Stone, R. G. 1970, *Solar Physics*, 15, 222
- Fleishman, G. D., Bastian, T. S., & Gary, D. E. 2008, *ASTROPHYSICAL JOURNAL*, 684, 1433
- Foullon, C., Fletcher, L., Hannah, I. G., et al. 2010, *The Astrophysical Journal*, 719, 151
- Glesener, L., Krucker, S., Duncan, J., et al. 2020, *The Astrophysical Journal*, 891, L34
- Harra, L., Brooks, D. H., Bale, S. D., et al. 2020, *Astronomy and Astrophysics*, submitted
- Hayes, L. A., Inglis, A. R., Christe, S., Dennis, B., & Gallagher, P. T. 2020, *ApJ*, 895, 50
- Hudson, H. S. 1991, *Solar Physics*, 133, 357
- Inglis, A. R., Ireland, J., & Dominique, M. 2015, *ApJ*, 798, 108
- Innes, D. E., Cameron, R. H., & Solanki, S. K. 2011, *Astronomy & Astrophysics*, 531, L13
- Ishikawa, S.-n., Glesener, L., Krucker, S., et al. 2017, *Nature Astronomy*, 1, 771
- Islaker, H., Vlahos, L., Benz, A., & Raoult, A. 1998, *Astronomy and Astrophysics*, 336, 371
- James, T., Subramanian, P., & Kontar, E. P. 2017, *Monthly Notices of the Royal Astronomical Society*, 471, 89
- Klimchuk, J. A. 2015, *Philosophical Transactions of the Royal Society A: Mathematical, Physical and Engineering Sciences*, 373, 20140256
- Knizhnik, K. & Reep, J. 2020, *Solar Physics*, 295
- Krupar, V., Szabo, A., Maksimovic, M., et al. 2020, *ApJS*, 246, 57
- Kumar, P., Nakariakov, V. M., & Cho, K.-S. 2016, *The Astrophysical Journal*, 822, 7
- Kumar, P., Nakariakov, V. M., & Cho, K.-S. 2017, *The Astrophysical Journal*, 844, 149
- Kupriyanova, E., Kolotkov, D., Nakariakov, V., & Kaufman, A. 2020, *Solar-Terrestrial Physics*, 6, 3
- Kupriyanova, E. G., Kashapova, L. K., Reid, H. A. S., & Myagkova, I. N. 2016, *Solar Physics*, 291, 3427
- Lemen, J. R., Title, A. M., Akin, D. J., et al. 2012, *Solar Physics*, 275, 17
- Li, H. D., Jiang, Y. C., Yang, J. Y., Bi, Y., & Liang, H. F. 2015, *Astrophysics and Space Science*, 359
- Liu, W., Jin, M., Downs, C., et al. 2018, *The Astrophysical Journal*, 864, L24
- Liu, W. & Ofman, L. 2014, *Solar Physics*, 289, 3233
- Liu, W., Zhao, J., Ofman, L., et al. 2011, *The Astrophysical Journal Letters*, 736, L13
- McClements, K. G. & Fletcher, L. 2009, *The Astrophysical Journal*, 693, 1494
- McIntosh, S. W. & De Pontieu, B. 2009, *The Astrophysical Journal*, 706, L80
- McLaughlin, J. A., Nakariakov, V. M., Dominique, M., JelÁnek, P., & Takasao, S. 2018, *Space Science Reviews*, 214
- McLaughlin, J. A., Verth, G., Fedun, V., & Erdélyi, R. 2012, *The Astrophysical Journal*, 749, 30
- Morioka, A., Miyoshi, Y., Masuda, S., et al. 2007, *The Astrophysical Journal*, 657, 567
- Murray, M. J., van Driel-Gesztelyi, L., & Baker, D. 2009, *Astronomy & Astrophysics*, 494, 329
- Nakariakov, V. M., Foullon, C., Verwichte, E., & Young, N. P. 2006, *ASTRONOMY & ASTROPHYSICS*, 452, 343
- Nakariakov, V. M. & Melnikov, V. F. 2009, *Space Science Reviews*, 149, 119
- Nakariakov, V. M. & Verwichte, E. 2005, *Living Reviews in Solar Physics*, 2
- Ofman, L. & Thompson, B. J. 2002, *The Astrophysical Journal*, 574, 440
- Parks, G. & Winckler, J. 1969, *The Astrophysical Journal*, 155, L117
- Pulupa, M., Bale, S. D., Badman, S. T., et al. 2020, *The Astrophysical Journal Supplement Series*, 246, 49
- Pulupa, M., Bale, S. D., Bonnell, J. W., et al. 2017, *Journal of Geophysical Research: Space Physics*, 122, 2836
- Roberts, B. 2000, *Solar Physics*, 193, 139
- Roberts, B., Edwin, P., & Benz, A. 1984, *The Astrophysical Journal*, 279, 857
- Schou, J., Scherrer, P. H., Bush, R. I., et al. 2012, *Solar Physics*, 275, 229
- Sych, R., Zaqarashvili, T. V., Nakariakov, V. M., et al. 2012, *Astronomy & Astrophysics*, 539, A23
- Sych, R., Zhugzhda, Y., & Yan, X. 2020, *The Astrophysical Journal*, 888, 84
- Thurgood, J. O., Pontin, D. I., & McLaughlin, J. A. 2017, *The Astrophysical Journal*, 844, 2
- Tun Beltran, S. D., Cutchin, S., & White, S. 2015, *Solar Physics*, 290, 2423
- Van Doorselaere, T., Kupriyanova, E. G., & Yuan, D. 2016, *Solar Physics*, 291, 3143
- Veronig, A., Messerotti, M., & Hanslmeier, A. 2000, *Astronomy & Astrophysics*, 357, 337, eprint: nlin/0207021
- Veronig, A. M., Gömöry, P., Kienreich, I. W., et al. 2011, *The Astrophysical Journal*, 743, L10
- Viall, N. M. & Klimchuk, J. A. 2011, *The Astrophysical Journal*, 738, 24
- Zhao, J., Felipe, T., Chen, R., & Khomenko, E. 2016, *The Astrophysical Journal Letters*, 830, L17
- Zharkova, V. V., Arzner, K., Benz, A. O., et al. 2011, *Space Science Reviews*, 159, 357